JACS
JOURNAL OF THE AMERICAN CHEMICAL SOCIETY
Article
pubs.acs.org/JACS

Systematic Approach in Designing Rare-Earth-Free Hybrid Semiconductor Phosphors for General Lighting Applications

Xiao Zhang,† Wei Liu,† George Z. Wei, Debasis Banerjee, Zhichao Hu, and Jing Li*

Department of Chemistry and Chemical Biology, Rutgers University, 610 Taylor Road, Piscataway, New Jersey 08854, United States

Supporting Information

ABSTRACT: As one of the most rapidly evolving branches of solid-state lighting technologies, light emitting diodes (LEDs) are gradually replacing conventional lighting sources due to their advantages in energy saving and environmental protection. At the present time, commercially available white light emitting diodes (WLEDs) are predominantly phosphor based (e.g., a yellow-emitting phosphor, such as cerium-doped yttrium aluminum garnet or (YAG):Ce^{3+}, coupled with a blue-emitting InGaN/GaN diode), which rely heavily on rare-earth (RE) metals. To avoid potential supply risks of these elements, we have developed an inorganic−organic hybrid phosphor family based on I−VII binary semiconductors. The hybrid phosphor materials are totally free of rare-earth metals. They can be synthesized by a simple, low-cost solution process and are easily scalable. Their band gap and emission energy, intensity, and color can be systematically tuned by incorporating ligands with suitable electronic properties. High quantum efficiency is achieved for some of these compounds. Such features make this group of materials promising candidates as alternative phosphors for use in general lighting devices.

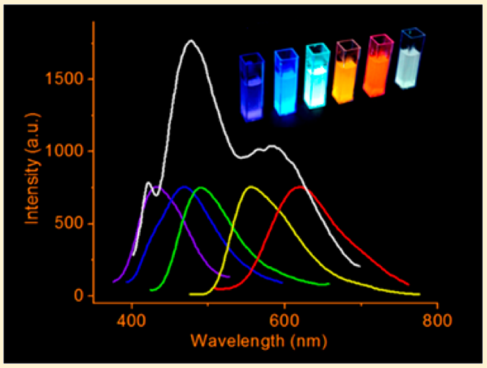

INTRODUCTION

Solid-state lighting (SSL) technology in the form of light-emitting diodes (LEDs) makes use of inorganic semiconductors to convert electricity to light. It is highly efficient, capable of converting energy much more effectively than conventional lighting sources. In addition to energy saving, it is also more environmentally friendly and, therefore, is being considered as a future-generation lighting technology.[1] The U.S. Department of Energy (DOE) has estimated that switching to LED lighting over the next two decades could save the country $250 billion in energy costs; this will reduce the electricity consumption for lighting by nearly one-half and decrease 1800 million metric tons of carbon emission.[2] The essential elements of LEDs are an electron-carrying n-layer and a hole-carrying p-layer. When a forward voltage is applied to the structure, electrons are injected from the n-layer and holes from the p-layer.[3] Electrons and holes can radiatively recombine, emitting a photon. The wavelength and color of the photon are determined by the difference in the energy levels of the electrons and holes.

LED technology has experienced rapid development since the 1970s. During the 1990s, three primary color (red, green, and blue) LEDs with high brightness were successfully produced.[4,5] Since then, LED devices have become viable choices for a variety of applications, ranging from monochrome signaling (e.g., traffic lights) to computer displays, and are now being considered as a potential source of white light to replace conventional lamps for general lighting purposes. Common approaches to produce white LEDs (WLEDs) include two methods. The first is to blend three primary color single-chip LEDs, namely red, green, and blue (RGB) diodes.[6−14] This process requires complex doping/mixing and delicate control of multiple materials and colors, which are both complex and costly. Presently, commercially available WLEDs are predominantly produced by a second method, namely phosphor-converted WLEDs or PC-WLEDs (e.g., a yellow-emitting phosphor, yttrium aluminum garnet or (YAG):Ce^{3+}, coupled with a blue-emitting InGaN/GaN diode).[15−17] While they are less expensive than the RGB diodes, the WLEDs made of (YAG):Ce^{3+} type phosphors have full dependence on rare-earth (RE) elements that are potentially facing a serious supply shortage, and their lack of recyclability is destructive to the environment. Today, about 20% of global RE elements are used in clean energy technologies. Among them, europium, terbium, and yttrium are essential ingredients of phosphors used in general lighting. Since the demand for RE elements will continue to increase dramatically for various technologies, their prices have been rising constantly, making the cost issue even more crucial.[18] Other issues of (YAG):Ce^{3+} type WLEDs range from unsuitability for solution processing to poor color rendering index (CRI) and high correlated color temperature (CCT). The deficiency in red emission is the main reason for their poor CRI and high CCT values, and as a result, they produce a colder and bluer white light in comparison to conventional incandescent bulbs.[19,20]

Received: August 2, 2014
Published: September 12, 2014

   dx.doi.org/10.1021/ja507927a | J. Am. Chem. Soc. 2014, 136, 14230−14236

Several RE-free white phosphors have been developed in recent years. Examples include ultrasmall nanocrystals of CdSe[21,22] and QDs with different colors.[23,24] However, low efficiency is usually unavoidable due to particle size variation, self-absorption, and quenching.[16] Inorganic−organic hybrid white phosphors such as (EDBE)[$PbBr_{4-x}Cl_x$] (EDBE = 2,2′-(ethylenedioxy)bis(ethylammonium)) and Cd_2Q_2(alkylamine) (Q = S, Se) have also been reported, though issues such as complicated synthetic procedure, low quantum efficiency,and color quality remain to be resolved.[25−27] On the basis of these considerations, it is clear that developing new phosphors that are RE free, cost effective, and solution processable and have improved quantum efficiency and color quality is not only of great need but is also a high priority. Here we report the rational design and synthesis of a CuI-based hybrid semiconductor family 1D-CuI(L) (1D = one-dimension, L = organic ligand) as alternative phosphors free of rare-earth elements. Our approach allows a systematic fine tuning of their band gaps and optical emissions to cover the entire visible range, including yellow and white colors. Due to the combination of these features, this material class shows significant promise for use in general lighting applications.

EXPERIMENTAL SECTION

Materials: CuI (98%, Alfa Aesar), acetonitrile (>99%, Alfa Aesar), pyridine (>99%, Alfa Aesar), 3,5-dimethylpyridine (>98%, Alfa Aesar), 4-picolone (99%. Alfa Aesar), 3-picoline (99%, Alfa Aesar), 2-ethyl-3-methylpyrazine (98%, Sigma-Aldrich), 3-bromopyridine (>98%, Alfa Aesar), 4-acetylpyridine (98%, Acros), 2,6-dimethylpyrizine (99%, Alfa Aesar), 5-bromopyrimidine (98%, Alfa Aesar), 2-cyanopyrazine (98%, Alfa Aesar), pyrimidine (98%, Alfa Aesar), pyrazine (98%, Alfa Aesar), KI (99%, Alfa Aesar).

Synthesis of 1D-CuI(4-pc) (1; 4-pc = 4-Picoline). The synthesis of 1D-CuI(4-pc) is based on a previously published procedure[28] with some modification. A solution (2 mL) of ethanol and 4-pc (0.093 g; 1 mmol) was slowly added to a saturated KI solution (2 mL) containing CuI (0.190 g; 1 mmol). Needlelike colorless crystals formed in 3 h. The product was collected by filtration and dried in the vacuum oven (65% yield). Powder samples were obtained by directly mixing a stoichiometric amount of CuI/saturated KI solution with 4-pc/ethanol solution at room temperature with magnetic stirring. A precipitate formed immediately and was collected by filtration.

Synthesis of 1D-CuI(3,5-dm-py) (2; 3,5-dm-py = 3,5-Dimethylpyridine). Single crystals of 1D-CuI(3,5-dm-py) were grown at room temperature by a new diffusion growth technique that we recently developed. A solution of CuI (0.190 g; 1 mmol) in saturated potassium iodide (KI) solution (2 mL) and a solution of 3,5-dm-py (0.108 g; 1 mmol) in acetone (2 mL) were separated by a layer of 2 mL of acetonitrile used as a middle layer. The mixture was left overnight, producing colorless needlelike crystals in 85% yield. Powder samples were obtained by adding a stoichiometric amount of 3,5-dm-py in ethanol solution to a CuI/saturated KI solution with magnetic stirring at room temperature. Note that excess ligand leads to the formation of a cubane-based structure.

Synthesis of 1D-CuI(3-pc) (3; 3-pc = 3-Picoline). Single crystals of 1D-CuI(3-pc) were obtained by a diffusion growth technique modified from published work.[28] A CuI/saturated KI solution was placed at the bottom of the reaction vessel, and 3-pc (0.093 g; 1 mmol) in 2 mL of acetone was placed on the top layer. The middle layer was acetonitrile, where the needlelike crystals formed over a period of 12 h (yield 91%). Pure phase powder samples were obtained by adding a deficient amount of 3-pc to the CuI/KI solution. An excess amount of 3-pc leads to the formation of a dimer-based product.

Synthesis of 1D-CuI(py) (4; py = Pyridine). 1D-CuI(py) was synthesized according to a previous report[29] with modification. A CuI solution (0.190 g; 1 mmol) prepared in saturated KI solution (2 mL) was placed at the top of a three-layer solution, followed by a layer of acetonitrile (2 mL) and a third layer of py (0.079 g; 1 mmol) in acetone (2 mL). Colorless needlelike crystals formed overnight in 74% yield. Pure powder samples were obtained by adding a deficient amount of py/ethanol solution into a CuI/KI solution. Excess py leads to the formation of cubane-based phases.

Synthesis of 1D-CuI(3-Br-py) (5; 3-Br-py = 3-Bromopyridine). Single crystals of 1D-CuI(3-Br-py) were acquired by reaction of a solution of CuI (0.190 g; 1 mmol) in saturated potassium iodide solution (2 mL) with a solution of 3-Br-py (0.158 g; 1 mmol) in acetone (2 mL). A 2 mL portion of acetonitrile was used as an interlayer between the above two solutions. The mixture was left at room temperature overnight, and the resulting colorless needlelike crystals were collected after filtration. The yield was 44%. Powder samples were synthesized by mixing stoichiometric CuI/saturated KI solution with 3-Br-py/ethanol solution at room temperature with magnetic stirring.

Synthesis of 1D-CuI(2-et-3-me-pz) (6; 2-et-3-me-pz = 2-Ethyl-3-methylpyrazine). Single crystals of 1D-CuI(2-et-3-me-pz) were grown by reacting CuI (0.190 g; 1 mmol) in saturated potassium iodide solution (2 mL) with 2-et-3-me-pz (0.122 g; 1 mmol) in ethanol (2 mL). A 2 mL portion of acetonitrile was used as an interlayer between the above two solutions. The reaction mixture was heated at 100 °C for 24 h and then cooled to room temperature. The product contains both powders and needleshaped crystals in a yield of 35%.

Synthesis of 1D-CuI(2,6-dm-pz) (7; 2,6-dm-pz = 2,6-Dimethylpyrazine). Single crystals of 1D-CuI(2,6-dm-pz) (**7**) were generated by the same layering method: a CuI solution and a 2,6-dimethylpyrazine (0.108 g; 1 mmol) solution in acetone (2 mL) were interlayered by 2 mL of acetonitrile. Reaction at room temperature overnight produced rod-shaped yellowish crystals of 1D-CuI(2,6-dm-pz) in a yield of 33%. Powder samples were synthesized by adding stoichiometric 2,6-dm-pz/ethanol to a CuI/saturated KI solution at room temperature. A yellow precipitate formed immediately.

Synthesis of 1D-CuI(5-Br-pm) (8; 5-Br-pm = 5-Bromopyrimidine). The crystal growth of 1D-CuI(5-Br-pm) (**8**) was essentially the same as that of 1D-CuI(3-Br-pm), except 5-Br-pm was used. Yellowish rodlike crystals of 1D-CuI(5-Br-pm) were collected after filtration (18% yield). Powder samples were prepared by adding stoichiometric 5-Br-pm/ethanol to a CuI/saturated KI solution at room temperature. A precipitate formed immediately. A longer reaction time would result in a dimer-based structure.

Synthesis of 1D-CuI(2-cy-pz) (9; 2-cy-pz = 2-Cyanopyrazine). The synthesis of compound **9** was carried out according to the literature.[30] A solution of CuI (0.191 g; 1 mmol) in acetonitrile was mixed with 2-cy-pz in CH_2Cl_2 (2 mL). The reaction mixture was heated at 120 °C for 6 h. Orange rod-shaped crystals and a powder sample were formed in 15% yield.

Synthesis of 1D-CuI(4-ac-py) (10; 4-ac-py = 4-Acetylpyridine). Single crystals of **10** were grown by a method that is different from the reported procedure.[31] A solution of CuI in the same quantity and concentration as those described previously was used to layer with a 4-ac-py (0.121 g; 1 mmol) solution of acetone (2 mL). Acetonitrile (2 mL) was used as the interlayer. Orange rod-shaped crystals grew slowly overnight and were collected after filtration. The yield was 80%. A powder sample was synthesized by mixing stoichiometric 4-ac-py/ethanol with CuI/saturated KI solution directly at room temperature. An orange powder formed immediately after mixing and was collected by filtration.

Synthesis of 1D-CuI$(py)_{1-x}(pm)_x$ Compounds (11). Powder samples of 1D-CuI$(py)_{1-x}(pm)_x$ (**11**) were prepared by adding py (0.128 g; 1.6 mmol) and pm (0.008 g; 0.1 mmol) in 3 mL of acetone drop by drop into a solution of CuI (0.191 g; 1 mmol) in 2 mL of saturated KI solution. A white powder of 1D-CuI$(py)_{1-x}(pm)_x$ immediately precipitated from the solution.

Solution Process of Samples for Coating. Fine powder samples were first dispersed in acetone under ultrasonication for 30 min to obtain a well-dispersed solution. The sample was then coated onto the targeted substrate by spaying the solution onto the substrate surface and letting it dry in the air.

dx.doi.org/10.1021/ja507927a | J. Am. Chem. Soc. 2014, 136, 14230−14236

Single-Crystal X-ray Diffraction (SXRD). Single-crystal X-ray diffraction data were collected at low temperature (100 K) on a Bruker-AXS Smart APEX CCD diffractometer with graphite-monochromated Mo Kα radiation (λ = 0.71073 Å). The structures were solved by direct methods and refined by full-matrix least squares on F^2 using the Bruker SHELXTL package. Crystal data of **2**: $C_7H_9N_2CuIN$, fw = 297.59, monoclinic, $C2/c$, V = 1768.4(10) Å^3, Z = 8, R1 = 0.0266, wR2 = 0.0644 ($I > 2\sigma(I)$), GOF = 1.037. Crystal data of **5**: $C_5H_4BrCuIN$, fw = 348.44, monoclinic, $P2_1/n$, Z = 8, R1 = 0.0423, $wR2$ = 0.1221 ($I > 2\sigma(I)$), GOF = 1.090. Crystal data of **6**: $C_7H_{10}N_2CuI$, fw = 312.61, triclinic, $P\bar{1}$, V = 467.4(4) Å^3, Z = 2, R1 = 0.0476, wR2 = 0.1007 ($I > 2\sigma(I)$), GOF = 1.007. Crystal data of **7**: $C_6H_6CuIN_2$, fw = 298.59, monoclinic, $P2_1/c$, V = 852.3(2) Å^3, Z = 4, R1 = 0.0369, wR2 = 0.0744 ($I > 2\sigma(I)$), GOF = 1.088. Crystal data of **8**: $C_4H_3BrCuIN_2$, fw = 349.43, monoclinic, $P2_1/c$, V = 1519.8(3) Å^3, Z = 8, R1 = 0.0326, wR2 = 0.756 ($I > 2\sigma(I)$), GOF = 1.010. These data can be obtained free of charge from the Cambridge Crystallographic Data Centre via www.ccdc.cam.ac.uk/data_request/cif. The structures were deposited in the Cambridge Structural Database (CSD), and the file numbers are 1013280−1013284. A brief summary of the crystal data of all five compounds are given in Table 1.

Table 1. List of New 1D-CuI(L) Compounds with Their Unit Cell Parameters and Space Groups

compd	unit cell constant (Å, deg)	space group
1D-CuI(3,5-dm-py) (**2**)	a = 14.103(5)	$C2/c$
	b = 15.401(5)	
	c = 8.219(3)	
	β = 97.846(4)	
1D-CuI(3-Br-py) (**5**)	a = 19.631(2)	$P2_1/n$
	b = 4.1503(5)	
	c= 20.210(2)	
	β = 106.168(2)	
1D-CuI(2-et-3-me-pz) (**6**)	a = 4.275(2)	$P\bar{1}$
	b = 8.235(4)	
	c = 13.887(7)	
	α = 103.630(6)	
	β = 90.623(6)	
	γ= 99.902(6)	
1D-CuI(2,6-dm-pz) (**7**)	a = 4.1415(7)	$P2_1/c$
	b = 27.341(5)	
	c = 7.5831(12)	
	β = 96.983(2)	
1D-CuI(5-Br-pm) (**8**)	a = 16.774(2)	$P2_1/c$
	b = 4.1600(5)	
	c = 21.793(3)	
	β = 92.017(2)	

Powder X-ray Diffraction (PXRD). PXRD patterns of all compounds were obtained from a Rigaku Ultima-IV automated diffraction system with Cu Kα radiation. Measurements were made in a 2θ range of 3−50°. The data were collected at room temperature with a step of 0.02° (2θ) and a counting time of 0.2 s/step. The operating power was 40 kV/44 mA.

Optical Diffuse Reflectance Measurements. Optical diffuse reflectance spectra were measured at room temperature on a Shimadzu UV-3600 spectrophotometer. Data were collected in the wavelength range 250−2000 nm. $BaSO_4$ powder was used as a standard (100% reflectance). A procedure similar to that previously described was used to collect and convert the data using the Kubelka−Munk function. The scattering coefficient (S) was treated as a constant, since the average particle size of the samples used in the measurements was significantly larger than 5 μm.

Thermogravimetric (TG) Analysis. TG analyses of the title compounds were performed on a computer-controlled TG Q5000IR analyzer (TA Instruments). Pure powder samples were loaded into platinum pans and heated with a ramp rate of 10 °C/min from room temperature to 400 °C.

Photoluminescence (PL) Emission Measurements. Photoluminescence measurements of powder samples were carried out on a Varian Cary Eclipse spectrophotometer at room temperature. Glass slides having no emission in the visible range were used sample holders with powder samples being uniformly coated.

Internal Quantum Yield Measurements. Internal quantum yields (QYs) of samples in powder form were measured on a C9920-03 absolute quantum yield measurement system (Hamamatsu Photonics) with a 150 W xenon monochromatic light source and 3.3 in. integrating sphere.

DFT Calculations. Band structure (BS) and density of states (DOS) calculations were performed on 1D-CuI(3,5-dm-py) (**2**) and 1D-CuI(py) (**4**) employing density functional theory (DFT)[32] (see Figure 1 and Figures S10−S15 (Supporting Information)). The

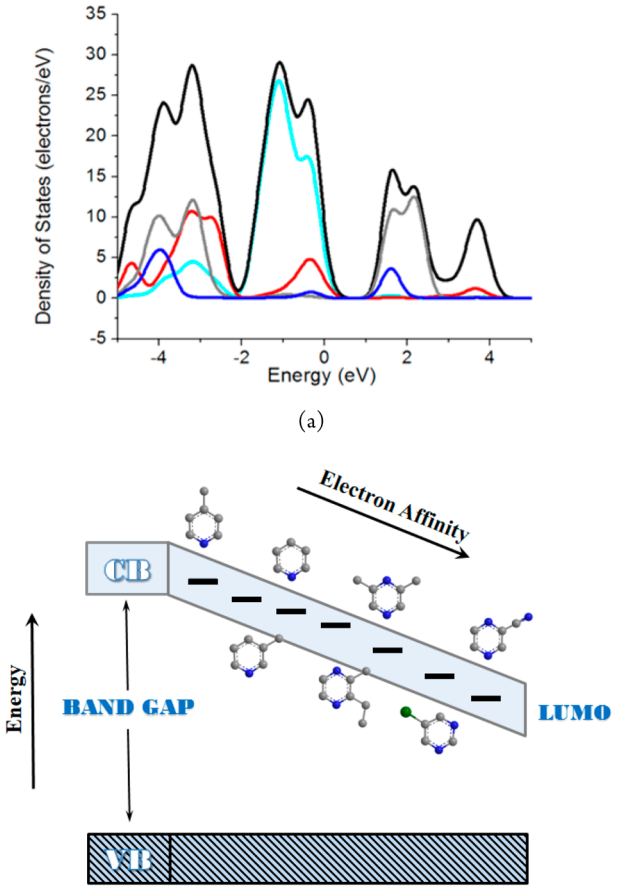

Figure 1. (a) Calculated density of states (DOS) of 1D-CuI(py) hybrid structure by DFT methods: (black) total DOS; (light blue) Cu 3d orbitals; (red) I 5p orbitals; (gray) C 2p orbitals; (blue) N 2p orbitals. (b) Schematic illustration showing the systematic tuning of band gap of 1D-CuI(L) hybrid structures by using ligands with different LUMO energies.

electronic properties of ligands were evaluated with density functional theory (DFT) computations using the Gaussian 09 suite of programs. A hybrid functional, B3LYP, was used for all calculations. Ligands were optimized using DGDZVP[33,34] and 6-31+G* basis sets, respectively.

RESULTS AND DISCUSSION

Crystalline inorganic−organic hybrid semiconductors are a very important and attractive material class that not only combine or

dx.doi.org/10.1021/ja507927a | J. Am. Chem. Soc. 2014, 136, 14230−14236

Table 2. Estimated Band Gaps, Emission Energies and Internal Quantum Yields (QYs), CIE Coordinates of 1D-CuI(L) Structures, and LUMO Energies of Organic Ligands Calculated at the B3LYP/6-311++G(3df,3pd) Level

compd	band gap (eV)	$\lambda_{em,max}$ (nm) (λ_{ex} 365 nm)	QY (%) (λ_{ex} 365 nm)	LUMO (eV)	CIE
1D-CuI(4-pc) (**1**)	3.2	433	35.8 ± 0.9	−0.96	0.20, 0.15
1D-CuI(3,5-dm-py) (**2**)	3.1	490	35.3 ± 0.7	−1.04	0.21, 0.36
1D-CuI(3-pc) (**3**)	3.0	469	37.2 ± 0.8	−1.07	0.19, 0.22
1D-CuI(py) (**4**)	2.9	475	29.1 ± 0.3	−1.12	0.20, 0.29
1D-CuI(3-Br-py) (**5**)	2.7	480	16.0 ± 0.7	−1.49	0.19, 0.23
1D-CuI(2-et-3-me-pz) (**6**)	2.6	490	32.4 ± 0.9	−1.49	0.23, 0.40
1D-CuI(2,6-dm-pz) (**7**)	2.4	525	15.4 ± 0.5	−1.61	0.35, 0.55
1D-CuI(5-Br-pm) (**8**)	2.3	545	13.1 ± 0.2	−1.97	0.46, 0.52
1D-CuI(2-cy-pz)(**9**)	2.2	618	10.1 ± 0.2	−2.80	0.55, 0.38
1D-CuI(py)$_{1-x}$(pm)$_x$ (**11**)	2.9	470, 590	12.5 ± 0.2		0.31, 0.33

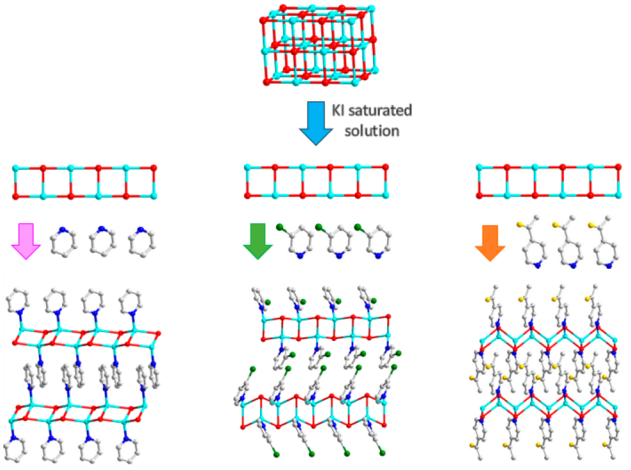

Figure 2. Design and construction of 1D-CuI(L) hybrid structures: (red ball) I; (light blue ball) Cu; (gray ball) C; (dark blue ball) N; (yellow ball) O. The inorganic 1D module is a CuI ribbon that can be regarded as a "cut" from the parent rock salt structure. The organic ligands bond to Cu metals in the chain via N atom and direct the formation of the crystal structure.

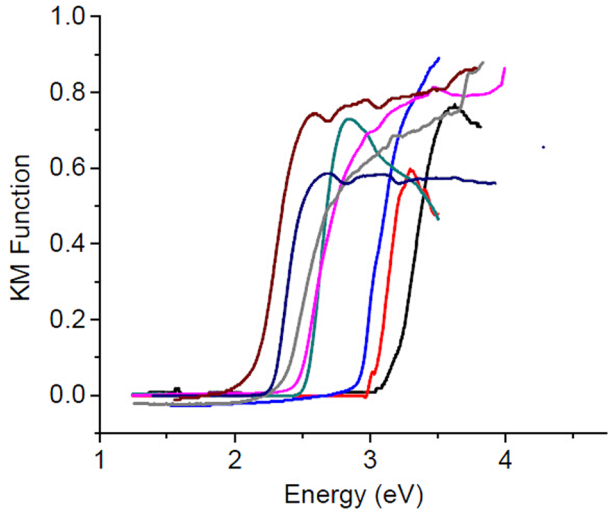

Figure 3. Optical absorption spectra of selected 1D-CuI(L) hybrid structures: (black) **1**; (red) **3**; (blue) **4**; (green) **6**; (pink) **7**; (gray) **8**; (dark blue) **9**; (brown) **10**.

enhance useful properties due to individual components[35−42] but also introduce unique and unprecedented features that are not possible by any constituent fragments, as a result of

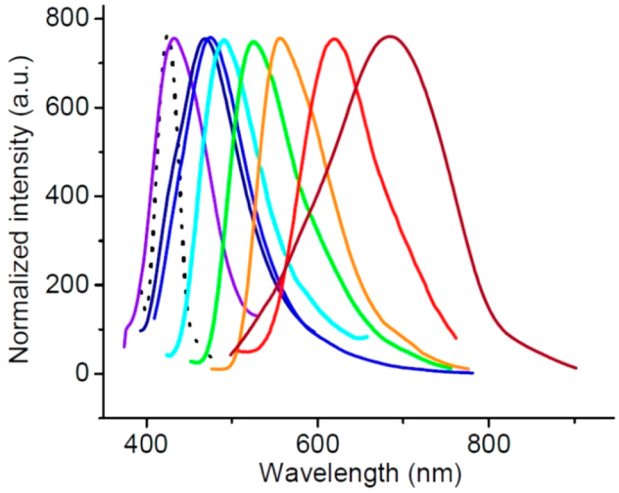

(a)

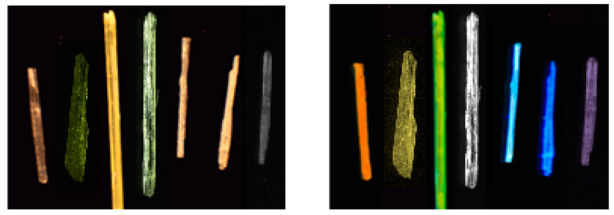

(b)

Figure 4. (a) Emission spectra of CuI semiconductor and selected 1D-CuI(L) hybrid structures (λ_{ex} 365 nm): (dotted black) bulk CuI; (purple) **1**; (dark blue) **3**; (blue) **4**; (cyan) **6**; (green) **7**; (orange) **8**; (red) **9**; (brown) **10**. (b) Selected crystal images of 1D-CuI(L) under daylight (left) and UV light (right; 365 nm). From left to right: **10**, **8**, **7**, **11**, **4**, **3**, **1**.

blending two very different species in a single crystal lattice.[26,35,43−49] In designing semiconductor-based hybrid phosphors, we have chosen the I−VII binary metal halides, because of their well-known and important optical properties,[50−55] and they were therefore chosen in this study as inorganic modules of the targeted hybrid phosphor compounds. Our DFT calculations on a prototype 1D-CuI(py) structure (see Figure 1) shows that the valence band maximum (VBM) is composed primarily of the inorganic module, namely Cu 3d and I 5p atomic orbitals, while the conduction band minimum (CBM) is made up dominantly of the LUMO orbital (C and N 2p atomic orbitals) of the organic ligands. This result suggests that it is possible to systematically tune the band gap

dx.doi.org/10.1021/ja507927a | J. Am. Chem. Soc. 2014, 136, 14230−14236

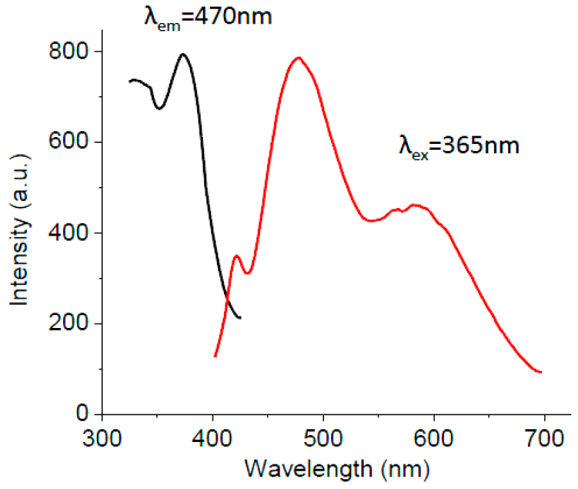

(a)

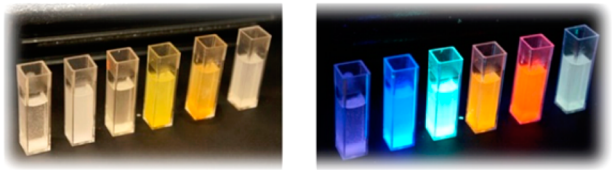

(b)

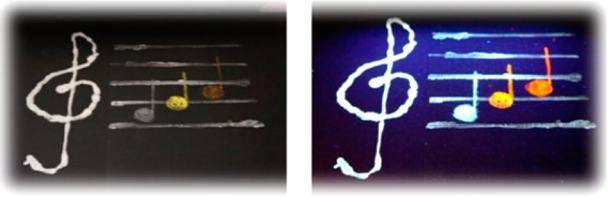

(c)

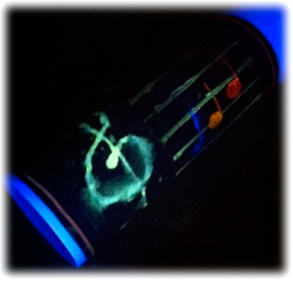

(d)

Figure 5. (a) Excitation spectrum (black, λ_{em} 470 nm) and PL emission spectrum (red, λ_{ex} 365 nm) of 1D-CuI(py)$_{1-x}$(pm)$_x$ (**11**). (b) Selected solution processed samples (from left to right: **1**, **3**, **6**, **8**, **9**, **11**) under daylight (left) and UV light (right, λ_{ex} 365 nm). (c) Solution-processed samples coated on paper under daylight (left) and UV light (right, λ_{ex} 365 nm). From left to right are **11** (the G clef), **3**, **8**, and **9** (the musical notes). (d) Sample-coated paper in (c) folded onto a cylinder (under UV light). Acetone was used as the solution for dispersion of the samples.

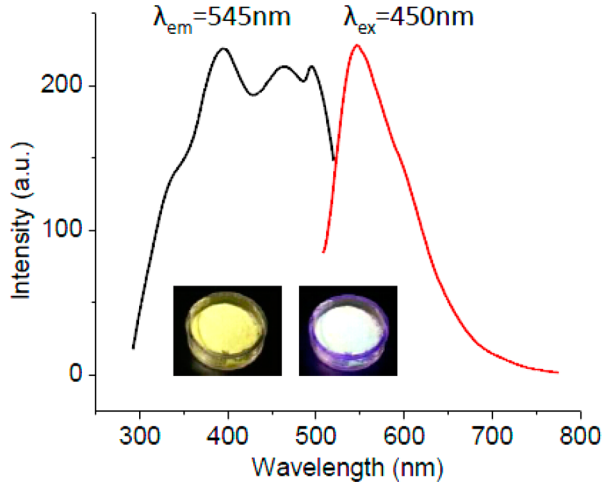

Figure 6. Excitation spectrum (black, λ_{em} 545 nm) and emission spectrum (red, λ_{ex} 450 nm) of 1D-CuI(5-Br-pm) (**8**). Inset: powder sample of **8** under natural light (left) and blue light (right, 450 nm).

of hybrid structures by selecting ligands with different LUMO energies, which in turn control the energy levels of the CBM (see Figure 1b). Employing DFT calculations, we then calculated LUMO orbitals of a number of pyridine-based ligands. The results are schematically illustrated in Figure 1b and given in Table 2. The general trend is that ligands containing electron-withdrawing groups give rise to low-lying LUMOs and those with electron-donating groups result in high-lying LUMOs.

Our synthesis was guided by the above findings. High-quality single crystals of a series of 1D-CuI(L) (L = organic ligand) hybrid structures were grown using a room-temperature diffusion method that we recently developed. In this method, reactants were dissolved in two different solvents and loaded in a reaction container as two separate layers. In most cases, a third solvent was selected to form an interlayer between the two to control the crystal growth rate. The crystal structures of these compounds were solved by single-crystal X-ray diffraction methods (see Table 1 and Table S1 (Supporting Information)).

All 1D-CuI(L) structures are built on Cu_2I_2 double-stranded one-dimensional chains which can be viewed as an electronically neutral infinite ribbon cut from the parent CuI rock salt type structure (see Figure 2). All organic ligands are pyridine-like or derivatives. They coordinate to the CuI 1D module via Cu−N bonds. In addition to the solution diffusion method developed for single-crystal growth, powder samples of 1D-CuI(L) hybrid compounds were prepared by simple, one-pot solution reactions at room temperature and their phase purity was examined by powder X-ray diffraction analysis (see the Experimental Section and Figures S6−S8 (Supporting Information)). Thermogravimetric (TG) analysis (see Figure S9 (Supporting Information)) confirmed that the experimental weight loss is in accordance with the calculated weight loss of each compound (loss of the ligand). Most of the compounds are stable up to 100−150 °C. These compounds are air and water stable. Both the structure and emission remain the same upon irradiation under a UV light source for several days.

Optical absorption spectra of selected 1D-CuI(L) hybrid structures are plotted in Figure 3. The estimated band gap values are given in Table 2. These values are fully in trend with the LUMO energies of the constituent ligands, confirming that the CBM and consequently the band gap of the 1D-CuI(L) family can be modulated by the choice of ligand. The decrease in the band gap from compound **1** to **9** follows the descending order of electron-donating ability of the corresponding ligands (4-pc > 3,5-dm-py > 3-pc > py > 3-Br-py > 2-et-3-me-pz > 2,6-

dx.doi.org/10.1021/ja507927a | J. Am. Chem. Soc. 2014, 136, 14230−14236

dm-pz > 5-Br-pm > 2-cy-pz) and, consequently, their LUMO energies (see Table 2).

The photoluminescence (PL) of these compounds is plotted in Figure 4a. Their emissions are quite different from those of the parent CuI semiconductor and organic ligands. CuI gives a sharp emission at ∼420 nm (see dotted black line in Figure 4a), and organic ligands typically either emit in the UV range (e.g., 5-Br-pm) or are not luminescent. For example, 1D-CuI(2,6-dm-pz) (7) emits at 525 nm, an energy much lower than that of CuI, while 2,6-dm-pz is nonemissive. The emissions of most hybrid compounds are in trend with their band gap values. The emission wavelengths (energies) of the hybrid structures range from violet (433 nm, ∼2.9 eV) to red (670 nm, ∼1.8 eV), spanning the entire visible region (Figure 4b). The results show that in general the emission wavelengths of these hybrid compounds can be tuned systematically by tailoring their band gaps. This can be achieved by choosing organic ligands with the desired electronic properties.

The internal quantum yields (QYs) were measured on a C9920-03 absolute quantum yield measurement system (Hamamatsu Photonics) at room temperature, and the values are given in Table 2. The highest value is obtained for 1D-CuI(3-pc) (**2**), ∼37.2%. In general, compounds containing electron-withdrawing groups have lower QYs, while those with electron-donating groups have higher QYs.

In order to achieve white light emission, we attempted to "dope" the 1D-CuI(L) structures with a second ligand. Pyridine was chosen as the primary ligand and pyrimidine as the dopant. PXRD analysis confirmed the phase purity of the doped products (**11**). As shown in Figure 5a, its emission properties are significantly different from that of the parent structure, 1D-CuI(py), exhibiting a much broader and more well balanced white emission with optimal CIE coordinates of (0.31, 0.33), calculated by GoCIE software, coincident with those of pure white light. The quantum yield of this compound is 12.5% under UV excitation (λ_{ex} 365 nm). The color rendering index (CRI) and correlated color temperature (CCT) are 87.4 and 6455 K, respectively. In comparison to YAG:Ce^{3+}, which usually has a CRI value of 70−80, this phosphor gives out a higher emission quality and warmer white light, as a result of its broader converge in the high-wavelength region. All samples can be processed in solution (Figure 5b) and readily coated on different types of substrates such as a flexible paper (Figure 5c,d).

In addition to white-emitting compound **11**, 1D-CuI(2,6-dm-pz) (7) and 1D-CuI(5-Br-pm) (**8**) both emit yellow light on excitation by a blue LED (450 nm), very similar to the case for the commercial yellow phosphor YAG:Ce^{3+} (Figure 6a). White light is generated by combining emission from a blue light source and yellow emission of the phosphor (see inset in Figure 6). The quantum yields of these two blue-excitable yellow phosphors are 18.9% and 8.0%, respectively, on excitation at 450 nm.

CONCLUSION

Guided by theoretical calculations, we have applied a systematic approach in designing and synthesizing a series of 1D-CuI(L) hybrid phosphors that are free of rare-earth elements and that emit over the entire visible spectrum, from red to blue. Their band gaps and optical absorption and emission properties can be systemically and deliberately tuned by incorporating organic ligands with different LUMO energies. White light emission is achieved by doping pm into the 1D-CuI(py) structure or by exciting yellow-emitting 1D-CuI(5-Br-pm) or 1D-CuI(2,6-dm-pz) with a blue light source. The new phosphors have the advantage of low-cost and room-temperature synthesis, solution processability, and total exclusion of rare-earth metals, making them promising candidates for general lighting applications.

ASSOCIATED CONTENT

Supporting Information

Figures and tables giving crystallographic data and atomic positions of new structures, powder XRD patterns of all compounds, and DFT calculation results. This material is available free of charge via the Internet at http://pubs.acs.org.

AUTHOR INFORMATION

Corresponding Author

*E-mail for J.L.: Jingli@rutgers.edu.

Author Contributions

†These authors contributed equally.

Notes

The authors declare no competing financial interest.

ACKNOWLEDGMENTS

Financial support from the National Science Foundation (Grant No. DMR-1206700) is gratefully acknowledged. W.L. would like to thank Benjamin J. Deibert for his assistance in some image work.

REFERENCES

(1) Pimputkar, S.; Speck, J. S.; DenBaars, S. P.; Nakamura, S. *Nat. Photonics* **2009**, *3*, 179.
(2) U.S. Department of Energy, http://www1.eere.energy.gov/buildings/ssl/.
(3) Solid-State Lighting, http://ssls.sandia.gov/.
(4) Bergh, A.; Craford, G.; Duggal, A.; Haitz, R. *Phys. Today* **2001**, *54*, 42.
(5) Kuo, C. P.; Fletcher, R. M.; Osentowski, T. D.; Lardizabal, M. C.; Craford, M. G.; Robbins, V. M. *Appl. Phys. Lett.* **1990**, *57*, 2937.
(6) Guo, N.; Huang, Y. J.; You, H. P.; Yang, M.; Song, Y. H.; Liu, K.; Zheng, Y. H. *Inorg. Chem.* **2010**, *49*, 10907.
(7) Piao, X. Q.; Horikawa, T.; Hanzawa, H.; Machida, K. *Appl. Phys. Lett.* **2006**, *88*, 161908.
(8) Setlur, A. A.; Heward, W. J.; Gao, Y.; Srivastava, A. M.; Chandran, R. G.; Shankar, M. V. *Chem. Mater.* **2006**, *18*, 3314.
(9) Su, L. T.; Tok, A. I. Y.; Boey, F. Y. C.; Zhang, X. H.; Woodhead, J. L.; Summers, C. J. *J. Appl. Phys.* **2007**, *102*, 083541.
(10) Uoyama, H.; Goushi, K.; Shizu, K.; Nomura, H.; Adachi, C. *Nature* **2012**, *492*, 234.
(11) Park, S.-I.; Xiong, Y.; Kim, R.-H.; Elvikis, P.; Meitl, M.; Kim, D.-H.; Wu, J.; Yoon, J.; Yu, C.-J.; Liu, Z.; Huang, Y.; Hwang, K.-c.; Ferreira, P.; Li, X.; Choquette, K.; Rogers, J. A. *Science* **2009**, *325*, 977.
(12) Reineke, S.; Lindner, F.; Schwartz, G.; Seidler, N.; Walzer, K.; Luessem, B.; Leo, K. *Nature* **2009**, *459*, 234.
(13) Sun, Y. R.; Giebink, N. C.; Kanno, H.; Ma, B. W.; Thompson, M. E.; Forrest, S. R. *Nature* **2006**, *440*, 908.
(14) Taniyasu, Y.; Kasu, M.; Makimoto, T. *Nature* **2006**, *441*, 325.
(15) Anikeeva, P. O.; Halpert, J. E.; Bawendi, M. G.; Bulovic, V. *Nano Lett.* **2007**, *7*, 2196.
(16) Li, Y. Q.; Rizzo, A.; Cingolani, R.; Gigli, G. *Adv. Mater.* **2006**, *18*, 2545.
(17) Nizamoglu, S.; Zengin, G.; Demir, H. V. *Appl. Phys. Lett.* **2008**, *92*, 031102.
(18) http://energy.gov/sites/prod/files/DOE_CMS2011_FINAL_Full.pdf (Critical Materials Strategy, U.S. Department of Energy, December 2011).

(19) Daicho, H.; Iwasaki, T.; Enomoto, K.; Sasaki, Y.; Maeno, Y.; Shinomiya, Y.; Aoyagi, S.; Nishibori, E.; Sakata, M.; Sawa, H.; Matsuishi, S.; Hosono, H. *Nat. Commun.* **2012**, DOI: 10.1038/ncomms2138.
(20) Shang, M. M.; Li, G. G.; Geng, D. L.; Yang, D. M.; Kang, X. J.; Zhang, Y.; Lian, H. Z.; Lin, J. *J. Phys. Chem. C* **2012**, *116*, 10222.
(21) Bowers, M. J., 2nd; McBride, J. R.; Rosenthal, S. J. *J. Am. Chem. Soc.* **2005**, *127*, 15378.
(22) Rosson, T. E.; Claiborne, S. M.; McBride, J. R.; Stratton, B. S.; Rosenthal, S. J. *J. Am. Chem. Soc.* **2012**, *134*, 8006.
(23) Farvid, S. S.; Wang, T.; Radovanovic, P. V. *J. Am. Chem. Soc.* **2011**, *133*, 6711.
(24) Nizamoglu, S.; Zengin, G.; Demir, H. V. *Appl. Phys. Lett.* **2008**, *92*, 031102.
(25) Dohner, E. R.; Jaffe, A.; Bradshaw, L. R.; Karunadasa, H. I. *J. Am. Chem. Soc.* **2014**, DOI: 10.1021/ja507086b.
(26) Ki, W.; Li, J. *J. Am. Chem. Soc.* **2008**, *130*, 8114.
(27) Roushan, M.; Zhang, X.; Li, J. *Angew. Chem., Int. Ed.* **2012**, *51*, 436.
(28) Cariati, E.; Bu, X. H.; Ford, P. C. *Chem. Mater.* **2000**, *12*, 3385.
(29) Eitel, E.; Oelkrug, D.; Hiller, W.; Strahle, J. *Z. Naturforsch., B* **1980**, *35*, 1247.
(30) Rossenbeck, B.; Sheldrick, W. S. *Z. Naturforsch., B* **1999**, *54*, 1510.
(31) Cariati, E.; Roberto, D.; Ugo, R.; Ford, P. C.; Galli, S.; Sironi, A. *Chem. Mater.* **2002**, *14*, 5116.
(32) Clark, S. J.; Segall, M. D.; Pickard, C. J.; Hasnip, P. J.; Probert, M. J.; Refson, K.; Payne, M. C. *Z. Kristallogr.* **2005**, *220*, 567.
(33) Godbout, N.; Salahub, D. R.; Andzelm, J.; Wimmer, E. *Can. J. Chem.* **1992**, *70*, 560.
(34) Sosa, C.; Andzelm, J.; Elkin, B. C.; Wimmer, E.; Dobbs, K. D.; Dixon, D. A. *J. Phys. Chem.* **1992**, *96*, 6630.
(35) Kagan, C. R.; Mitzi, D. B.; Dimitrakopoulos, C. D. *Science* **1999**, *286*, 945.
(36) Mitzi, D. B. *Adv. Mater.* **2009**, *21*, 3141.
(37) Huang, X. Y.; Li, J.; Zhang, Y.; Mascarenhas, A. *J. Am. Chem. Soc.* **2003**, *125*, 7049.
(38) Zhang, Q. C.; Bu, X. H.; Lin, Z.; Wu, T.; Feng, P. Y. *Inorg. Chem.* **2008**, *47*, 9724.
(39) Huang, X. Y.; Li, J. *J. Am. Chem. Soc.* **2007**, *129*, 3157.
(40) Zhang, X.; Hejazi, M.; Thiagarajan, S. J.; Woerner, W. R.; Banerjee, D.; Emge, T. J.; Xu, W. Q.; Teat, S. J.; Gong, Q. H.; Safari, A.; Yang, R. G.; Parise, J. B.; Li, J. *J. Am. Chem. Soc.* **2013**, *135*, 17401.
(41) Wu, T.; Bu, X. H.; Liao, P. H.; Wang, L.; Zheng, S. T.; Ma, R.; Feng, P. Y. *J. Am. Chem. Soc.* **2012**, *134*, 3619.
(42) Gao, M. R.; Yao, W. T.; Yao, H. B.; Yu, S. H. *J. Am. Chem. Soc.* **2009**, *131*, 7486.
(43) Zhang, R. B.; Emge, T. J.; Zheng, C.; Li, J. *J. Mater. Chem. A* **2013**, *1*, 199.
(44) Huang, X. Y.; Roushan, M.; Emge, T. J.; Bi, W. H.; Thiagarajan, S.; Cheng, J. H.; Yang, R. G.; Li, J. *Angew. Chem., Int. Ed.* **2009**, *48*, 7871.
(45) Fu, H. X.; Li, J. *J. Chem. Phys.* **2004**, *120*, 6721.
(46) Fluegel, B.; Zhang, Y.; Mascarenhas, A.; Huang, X.; Li, J. *Phys. Rev. B* **2004**, *70*, 205308.
(47) Roushan, M.; Zhang, X.; Li, J. *Angew. Chem., Int. Ed.* **2012**, *51*, 436.
(48) Yao, W. T.; Yu, S. H.; Huang, X. Y.; Jiang, J.; Zhao, L. Q.; Pan, L.; Li, J. *Adv. Mater.* **2005**, *17*, 2799.
(49) Yao, H. B.; Gao, M. R.; Yu, S. H. *Nanoscale* **2010**, *2*, 323.
(50) Mitra, A.; Lucas, F. O.; O'Reilly, L.; McNally, P. J.; Daniels, S.; Natarajan, G. *J. Mater. Sci.: Mater. Electron.* **2007**, *18*, S21.
(51) Hwang, L. C.; Wei, T. H.; Hsia, Y. L.; Li, C. M.; Tu, P. L.; Wen, T. C. *J. Chin. Chem. Soc.* **2006**, *53*, 1235.
(52) Gaponenko, S. V. *Semiconductors* **1996**, *30*, 315.
(53) O'Reilly, L.; Natarajan, G.; McNally, P. J.; Cameron, D.; Lucas, O. F.; Martinez-Rosas, M.; Bradley, L.; Reader, A.; Daniels, S. *J. Mater. Sci.: Mater. Electron.* **2005**, *16*, 415.
(54) Milyukov, E. M. *J. Opt. Technol.* **1996**, *63*, 904.
(55) Ahn, D.; Chuang, S. L. *Appl. Phys. Lett.* **2013**, *102*, 121114.